Application of Spherical Copper Oxide (II) Water Nano-fluid as a Potential Coolant in a Boiling Annular Heat Exchanger

V. Nikkhah, M. M. Sarafraz, and F. Hormozi

Faculty of Chemical, Petroleum and Gas Engineering,
Semnan University, Semnan, Iran

Convective boiling heat transfer coefficient of spherical CuO (II) nanoparticles dispersed in water is experimentally quantified inside the vertical heat exchanger. Influence of different operating parameters including applied heat and mass fluxes, sub-cooling temperature and concentration of nano-fluid on forced convection and nucleate boiling heat transfer mechanisms is experimentally investigated and briefly discussed. Results show that by increasing heat and mass fluxes, the heat transfer coefficient considerably increases for both heat transfer regions, while by increasing the nanoparticle weight concentration, the heat transfer coefficient increases in convective heat transfer (about 35 % at the maximum concentration) and deteriorates the heat transfer coefficient (about 9 % at maximum concentration) in nucleate boiling region due to the formation of nanoparticle deposition on heating surface. Experimental results are then compared to well-known correlations. Results of comparisons reveal good agreement between experimental data and those obtained by some correlations. In addition, thermo-physical properties of CuO nano-fluid are experimentally measured and represented, which are a good reference for other nano-fluid-related studies.

Key words:

convection, nucleate boiling, nano-fluids, heat transfer enhancement, heat transfer deterioration

Introduction

Transferring a large amount of energy to/from a system has always been a challenge in cooling/heating systems as well as power cycles and refrigerants. Boiling phenomena is a key method for removing the heat from the high heat flux mediums and surfaces. Compared with convective heat transfer mechanism, boiling flows represent higher heat transfer coefficients and better thermal performances. Consequently, boiling systems are widely used for quenching the high heat flux reactors and some other high-thermal heating tools. Industrial tools can be designed efficiently if the boiling mechanism and its sub-phenomena are known in detail, which consequently improves the thermal efficiency and reduces the designed size of any type of industrial heat exchanger. Thus, specific attention should be dedicated to the enhancement of heat transfer coefficient. Nano-fluid is an engineered colloidal suspension of nano-sized particles in a base fluid, such as water or glycols, which provides special heat transfer features, such as enhancement of thermal conductivity and changing of the heat transfer surface due to scale formation. Enhance-

ments in boiling heat transfer processes are vital, and could make the aforementioned typical industrial applications more energy-efficient. The intensification of heat-transfer processes and the reduction of energy losses are hence important tasks, particularly with regard to the prevailing energy crisis[1,2]. Many investigators have been trying to develop/redevelop more efficient heat-transfer fluids and devices in micro/macro/meso sizes[3]. Among these researches, convective boiling has been more popular due to the requirement of industrial or electronically high heat flux chipset or circuits, which need to be chilled by employing convective fluids[4]. Since Faulkner et al. conducted an experiment to investigate the influence of ceramic nanoparticles on convective heat transfer coefficient in a plenary heat sink, and reported limited improvement of heat transfer coefficient, many researchers started to employ nano-fluid as a coolant inside the heat exchangers and heat transfer systems[5]. Lee and Mudawar used the Al_2O_3 nanoparticles in water to make nano-fluids to influence the operating parameters inside the microchannels in single and two-phase flow[6]. Critical Heat Flux (CHF) augmentation was reported, as well as scale formation and nanoparticle agglomerations inside the microchannel. Peng et al., Bouddouh, Kim et al. investigated the convective heat transfer of nano-fluid inside dif-

ferent systems and reported the increase of heat transfer coefficient when concentration of nano-fluids increased[7–11]. SiO$_2$ and CuO nano-fluid was tested by Henderson *et al.* who reported the controversial results based on deterioration of convective heat transfer coefficient of R-134a-based nano-fluid[12]. Limited application of nano-fluids was demonstrated by Das *et al.,* due to deposition of the nano-fluids on the heating surface, which caused the heat transfer coefficient of nucleate boiling region to significantly deteriorate[13]. Recently, Ahn *et al.* and Sarafraz *et al.* in their experiments showed that using the nano-fluid can enhance the convective and nucleate heat transfer boiling due to increased wettability of the surface as well as thermal conductivity of the fluid[14–16].

After publishing our previous works[17–19], we were determined to investigate the convective boiling heat transfer of stabilized dilute CuO$_2$ or CuO (II) water-based nano-fluid as a possible coolant inside the annular heat exchanger. Likewise, thermal properties of the CuO (II) nano-fluid are experimentally measured and represented. Influence of different operating parameters such as heat flux (0–175 kW m^{-2}), mass flux (350–1060 kg m^{-2} s^{-1}), and weight percentages of 0.1- 0.4 on the heat transfer coefficient in both heat transfer regions (forced convection and nucleate boiling) is experimentally investigated. For validating the experiments, comparisons between well-known convective and boiling correlations against the experimental data are carried out. It is also shown that if the nano-fluid is stable, significant enhancement of heat transfer coefficient in the region with heat transfer dominant mechanism of forced convection can be seen.

Experimental

Experimental setup

Fig. 1 schematically shows the test loop used for the experiments. The working fluid enters the loop from a main tank through the insulated pipes and is continuously circulated by a centrifugal pump (DAB Co.). Due to the importance of fluid flow rate in flow boiling heat transfer, a Flownetix ultrasonic flow meter is mounted in line of fluid to measure the flow rate with the least possible uncertainty. Also, a rotameter is installed at the outlet line of condenser to validate the flow rate values measured by ultrasonic device. The fluid temperature was measured by two PT-100 thermometers installed in two thermo-wells located before and after the annular test section. The complete cylinder was made from stainless steel 316a. Thermometer voltages, current and voltage drop from the test heater were all measured and processed using a data acquisition

system in conjunction with a PID temperature controller. The test section shown in Fig. 1 consists of an electrically heated cylindrical DC bolt heater (manufactured by Cetal Co.) with a stainless steel surface, which is mounted concentrically within the surrounding pipe. The dimensions of the test section are: diameter of heating rod, 22 mm; annular gap diameter (hydraulic diameter) 30 mm; length of the Pyrex tube is 400 mm; length of stainless steel rod, 300 mm; length of heated section, 140 mm, which means that just the first 140 mm of stainless steel is heated uniformly and radially by the heater. The axial heat transfer through the rod can be ignored according to the insulation of the both ends of the heater. The heat flux and wall temperature can be as high as 175,000 W m^{-2} and 163 °C, respectively. The local wall temperatures were measured with four stainless steel sheathed K-type thermocouples installed close to the heat transfer surface. The temperature drop between the thermocouples location and the heat transfer surface can be calculated from:

$$T_w = T_{th} - \dot{q}\,\frac{s}{\lambda_w} \tag{1}$$

The ratio between the distance of the thermometers from the surface and the thermal conductivity of the tube material ($s\,\lambda_w^{-1}$) was determined for each K-type thermocouple by calibration using Wilson plot technique[20]. The calibration temperature was 303 K according to Wilson technique. The average temperature difference for each test section was the arithmetic average of the four thermometer readings around the rod circumference. The average of 10 voltage readings was used to determine the difference between the wall and bulk temperature for each thermometer. All the K-type thermocouples were thoroughly calibrated using a constant temperature water bath, and their accuracy was estimated at ±0.3 K. The local heat transfer coefficient α is then calculated from:

$$\alpha = \frac{\dot{q}}{\left(T_w - T_b\right)_{ave.}} \tag{2}$$

To minimize the thermal contact resistance, high quality silicone paste was injected into the thermocouple wells. To avoid possible heat loss, main tank circumferences were heavily insulated using industrial glass wool. To control the fluctuations due to the alternative current, a regular DC power supply was also employed to supply the needed voltage to central heater. Likewise, to visualize the flow and boiling phenomenon and record the proper images, annulus was made of the Pyrex glass. Also, this apparatus is capable of measuring the pressure drop of test section using pressure sensors installed at the inlet and outlet of test section. However, pressure drop is not related to the goal of this work.
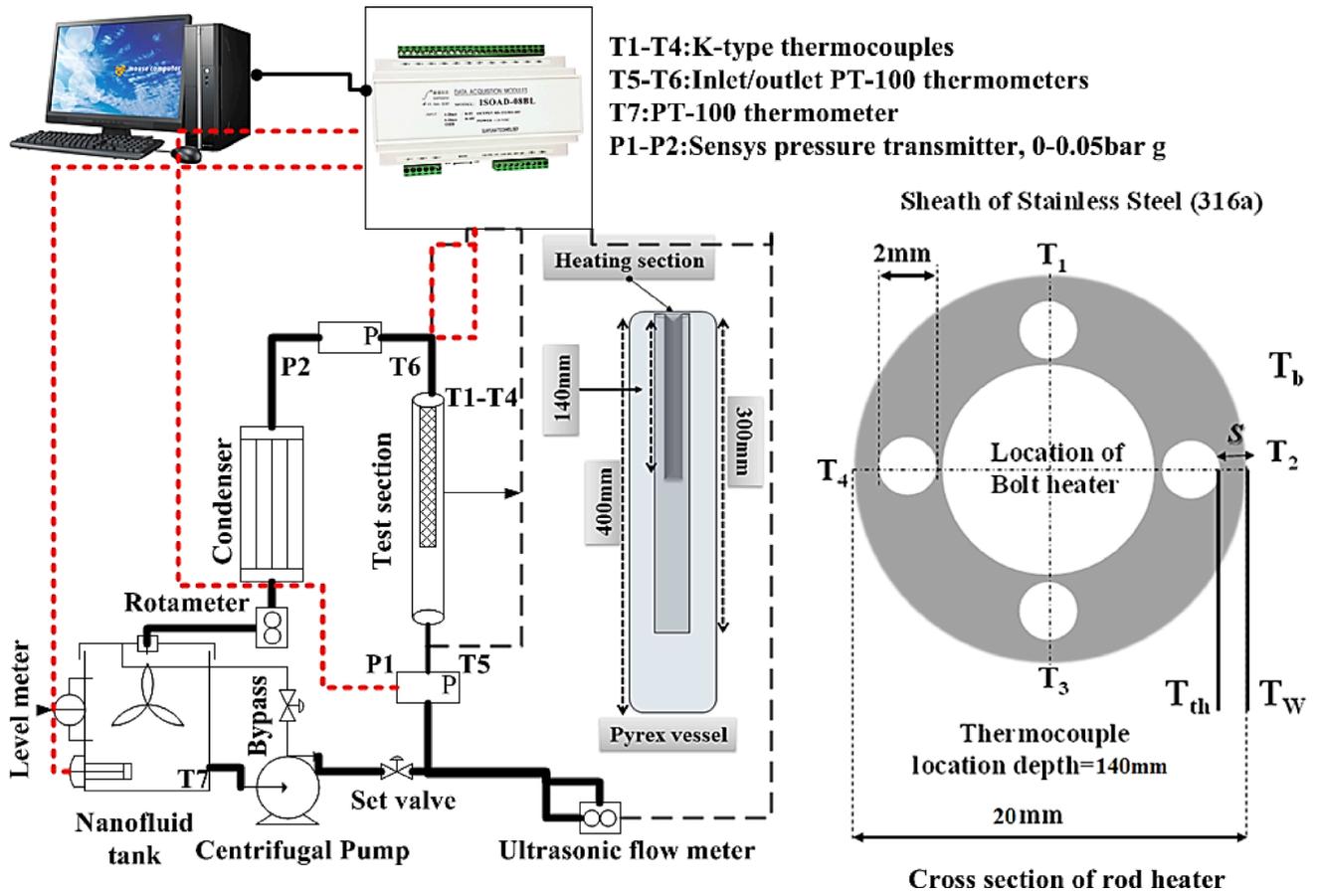
T1-T4:K-type thermocouples
T5-T6:Inlet/outlet PT-100 thermometers
T7:PT-100 thermometer
P1-P2:Sensys pressure transmitter, 0-0.05bar g

F i g . 1 – *Scheme of test loop*

Uncertainty analysis

The uncertainties of the experimental results are analyzed by the procedures proposed by Kline and McClintock[21]. The method is based on careful specifications of the uncertainties in the various primary experimental measurements. The heat transfer coefficient can be obtained using Eq. (3):

$$\alpha = \frac{\rho_{nf} V C_{pnf} (T_{out} - T_{in})}{(T_w - T_b)_{av.}} \quad (3)$$

As seen from Eq. (3), the uncertainty in the measurement of the heat transfer coefficient can be related to the errors in the measurements of volume flow rate, hydraulic diameter, and all the temperatures as follows.

$$\partial\alpha = \sqrt{\begin{aligned}&\left[\left(\frac{\partial\alpha}{\partial V}\right)\cdot\delta V\right]^2 + \left[\left(\frac{\partial\alpha}{\partial A}\right)\cdot\delta A\right]^2 + \\ &+\left[\left(\frac{\partial\alpha}{\partial(Tout-Tin)}\right)\cdot\delta(Tout-Tin)\right]^2 + \\ &+\left[\left(\frac{\partial\alpha}{\partial(Tw-Tb)}\right)\cdot\delta(Tw-Tb)\right]^2\end{aligned}} \quad (4)$$

According to the above uncertainty analysis, the uncertainty in the measurement of the heat transfer coefficient is 16.2 %. More information about the experimental setup as well as calibration method may be found in our previous studies[22–24]. The detailed results from the present uncertainty analysis for the experiments conducted here are summarized in Table 1. The main source of uncertainty is due to the temperature measurement and its related devices.

T a b l e 1 – *Summary of the uncertainty analysis*

Parameter	Uncertainty
Length, width and thickness, (m)	$\pm 5 \cdot 10^{-5}$
Temperature, (K)	± 0.3 K
Water flow rate, (L min^{-1})	± 1.5 % of readings
Voltage, (V)	± 1 % of readings
Current, (A)	± 0.02 % of readings
Cylinder side area, (m²)	$\pm 4 \cdot 10^{-8}$
Flow boiling heat transfer coefficient, (W m² K^{-1})	± 16.2 %

Stability and characterization of nano-fluids

Before running the experiments, the nano-fluids were prepared and stabilized using pH control and time-sedimentation experiments. In the present work, CuO nanoparticles (40–50 nm, Plasma Chem GmbH, Germany) were dispersed in deionized water as the base fluid. To check the quality, morphology and purity of nanoparticles, quality tests were performed. Results of quality tests can be seen in Figs. 2(a-c). As can be seen in Fig. 2a, XRD pattern depicts the single-phase CuO with a monoclinic structure which implies that there is no impurity other than CuO nanoparticles, and no significant peaks of impurities are found in XRD pattern. The peaks are broad due to the nano-size effect. In fact, similar to light and mirror, the particles are mainly responsible for the diffraction/reflection of X-ray test. In case of light and mirror, when the size of the mirror is small, the intensity of reflected light is low. Similarly, in X-ray physics the crystallite size is inversely proportional to the full width at half maximum of the diffraction peak (Scherer's formula), hence small particles or crystallites generally produce broader peaks. More information can be found in literature[19]. X-ray diffraction is one of the most important characterization tools, which is widely used in solid state chemistry and powder/particle sciences. This technology is an easy tool to determine the size and shape of particles and Phase Identification Quantitative analysis (PIQ). XRD pattern gives information on symmetry size and shape of the particle and purity of particles from peak positions. These peaks can be compared to those obtained for particular particles or powder and shape or impurity, and nano-size particles can be detected as well. It also gives information on deviations from a perfect particle. Fig. 2b demonstrates the particle size distribution of nano-fluid. As can be seen, the dominant size of particles is 50 nm and no clusters or aggregations with secondary particle size can be seen. Fig. 2c depicts the TEM image of CuO nanoparticles. As can be seen, CuO (II) nano-particles shapes are spherical and uniform in size. Noticeably, the dominant size of the nanoparticles is 40–50 nm, which is in accordance with nanoparticle size count test.

The two-step method was employed for preparing the nano-fluid. Briefly, the preparation process included: 1) Weigh the mass of CuO (II) with digital electronic balance. 2) The CuO (II) nanoparticle was added into the deionized water, while it was agitated in a flask. The magnetic motorized stirrer (Hanna Instruments Co.) was employed to agitate the nanoparticle inside the base fluid. 3) UP400S ultrasonic Hielscher GmbH (350 W/24 kHz) was used to disperse the nanoparticles into the water uniformly. The stabilization process was then car-
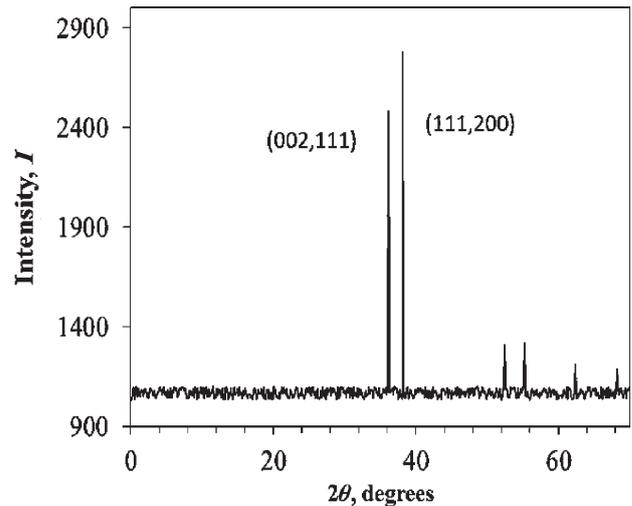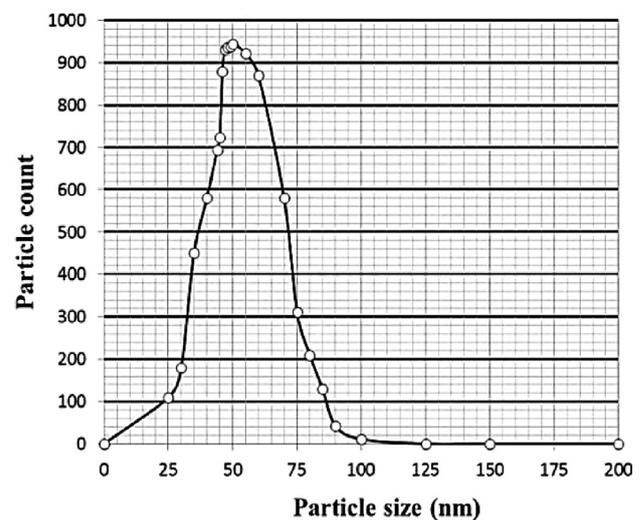

Fig. 2a – *XRD pattern of CuO (II) nanoparticles*
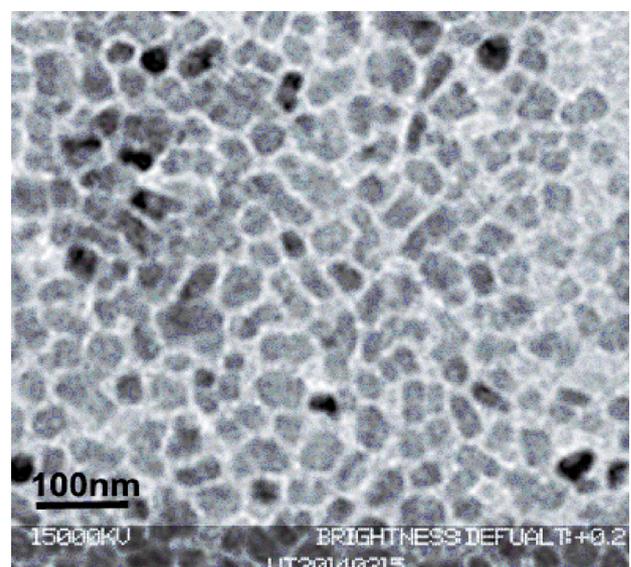

Fig. 2b – *Results of nanoparticle size count*

Fig. 2c – *TEM image of CuO (II) nanoparticles*

F i g . 3 – *Stability of CuO nano-fluid using pH control, stirring and sonication process*

ried out. Results of this experiment demonstrate that dilute CuO/water nano-fluid can be stabilized up to 1080 h using controlled pH equal to 10.2. Noticeably, to control the pH, dilute HCl and NaOH solution was used, since it has the least possible effect on thermo-physical properties of nano-fluids. Fig. 3 shows the stabilized nano-fluid at weight fraction of 0.004. Final results of pH control can be seen in Fig. 4. Stirring was performed at speed of 300 rpm for about 120 min. Sonication was performed for about 180 min.
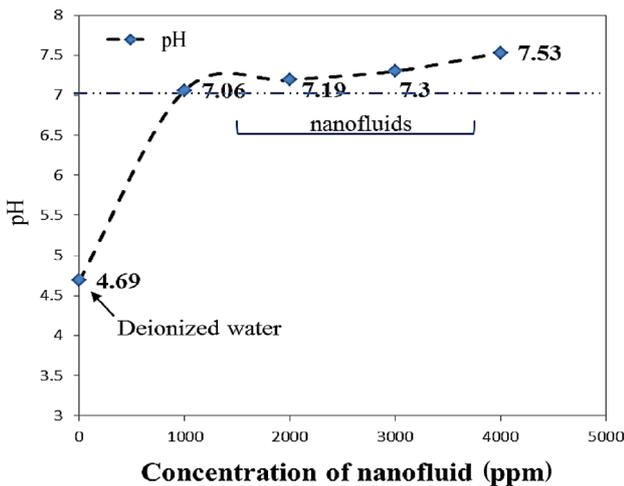
F i g . 4 – *pH of prepared nano-fluids*

Newtonian behavior and thermo-physical properties of nano-fluids

Convective heat transfer coefficient of nano-fluids strongly depends on the thermo-physical properties of the nanoparticles added to the base fluid and the type of fluid behavior (Newtonian/

none-Newtonian behavior). In the present work, thermal properties of CuO (II) nano-fluid were experimentally measured. These physical properties include: density, viscosity, thermal conductivity. Also, to check the Newtonian behavior of the nano-fluid, shear stress was experimentally measured and reported. As can be seen in Figs. 5 and 8, for the entire range of nano-fluid concentrations, by increasing the temperature, the density and viscosity of the nano-fluids decrease, while thermal conductivity of nano-fluids considerably increases (see Fig. 7). Likewise, Fig. 6 shows that nano-fluids have Newtonian behavior in temperature ranges of 303 K to 313 K, noticeably, when needed, thermo-physical properties can also be estimated using Table 2 correlations.
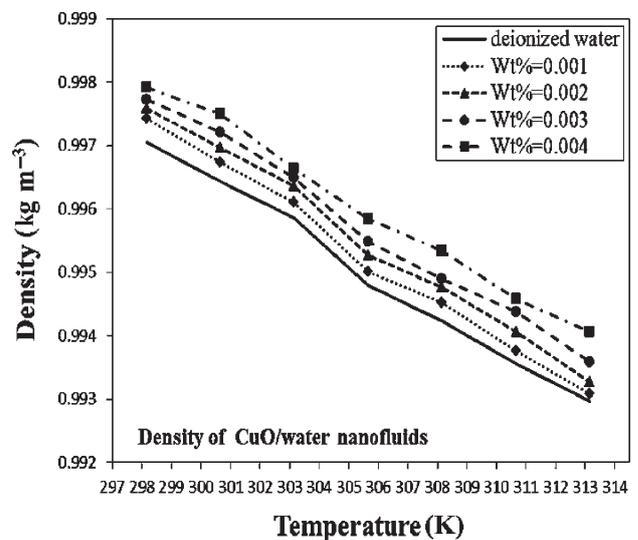

F i g . 5 – *Variation of density of CuO/water nano-fluid with temperature*

Table 2 – *Correlations for predicting the thermo-physical properties of nano-fluids[34]*

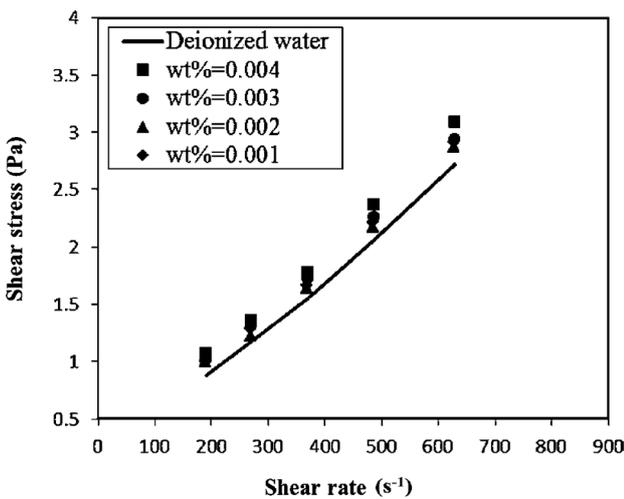| Physical properties	Correlation
Density	$\rho_{nf} = \varphi \rho_p + (1-\varphi) \rho_{bf}$
Heat capacity	$C_{pnf} = (1-\varphi)(\dfrac{\rho_{bf}}{\rho_{nf}}) C_{pnf} + \varphi(\dfrac{\rho_p}{\rho_{nf}}) C_{p_p}$
Viscosity	$\mu_{nf} = A(\dfrac{1}{T}) - B$ $A = 20587\varphi^2 + 15857\varphi + 1078.3$, $B = -107.12\varphi^2 + 53.548\varphi + 2.8715$
Thermal conductivity	$K_{nf} = \dfrac{K_p + (n-1)K_{bf} - \varphi(n-1)(K_{bf}-K_p)}{K_p + (n-1)K_{bf} + \varphi(K_{bf}-K_p)} K_{bf} + 50000 \cdot \beta\varphi\rho_{bf}C_{pbf} \cdot \Pi$ $\Pi = \sqrt{\dfrac{\kappa T}{\rho_p d_p}} f(T,\varphi)$ $f(\varphi,T) = 0.028217 \cdot \varphi + 0.003917(\dfrac{T}{T_0}) - 0.0030669\varphi - 0.003911$ For CuO (II) nano-particle: $\beta = 9.881(100\varphi)^{-0.9446}$ $n = \dfrac{3}{\phi}$, ϕ : Sphericity of nanoparticles

Fig. 6 – *Shear stress versus shear rate; nano-fluids are showing the Newtonian behavior*

Fig. 7 – *Variation of thermal conductivity of CuO/water nano-fluid with temperature*

Noticeably, viscosity of nano-fluids was measured using DV-II+ PRO digital viscometer (manufactured by Brookfield Co., accuracy: ±1.0 % of reading/ Repeatability: ±0.2 %). Density was also measured using DMA 4500 ME (manufactured by Anton Paar Co., accuracy: ±1.0 % of reading/Repeatability: 0.00001 g cm⁻³). Thermal conductivity was also measured using DTC300 (manufactured by TA Instrument, accuracy: ±3 % to 8 % depending on thermal resistance/ Repeatability: ±1 to ±2 % depending on thermal resistance/Standard: ASTM E1530). Distilled water was used as a calibration fluid to check the reliability and accuracy of experimental setup, because its thermo-physical properties are well-known and reach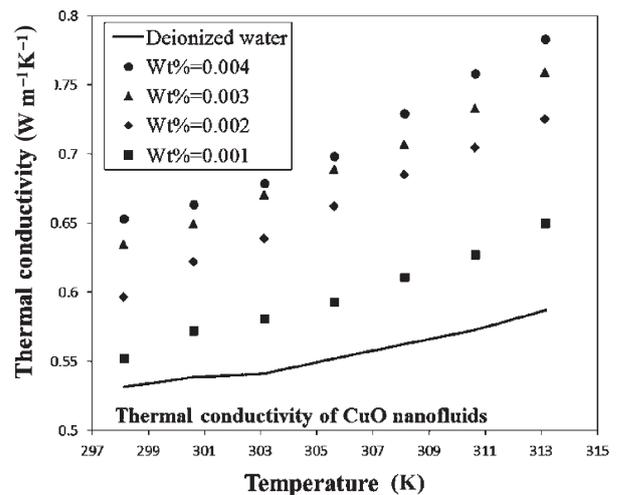able with high accuracy. The obtained results were then compared to Dittus-Boelter[25] correlation and Gnielinski[26] for laminar (A.A.D% of 12.1 %) and turbulent (A.A.D% of 4.1 %) regions respectively. These correlations are represented in detail in Table 3.

Fig. 9 shows the results of comparison between experimental data and those obtained by well-known correlations for deionized water and for different flow regimes.

In the following sections, the influences of operating parameters are experimentally investigated.

Influence of heat and mass fluxes

According to the experimental data, heat and mass flux have a strong effect on convective boiling

Table 3 – *Gnielinski and Dittus-Boelter correlations*

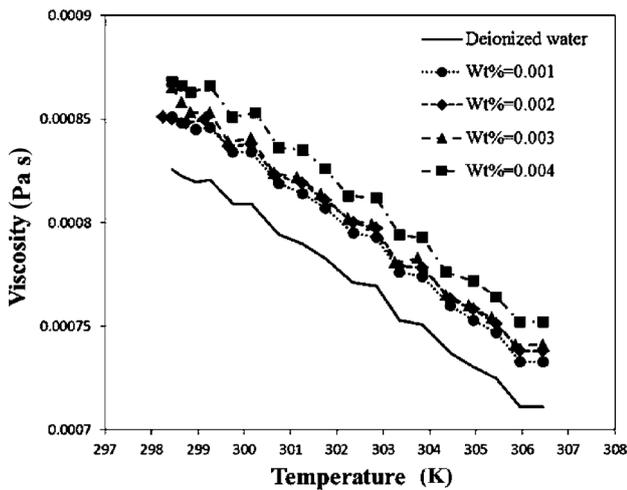| Correlation	Operating condition (this work)	Absolute average deviation	Flow regime
Dittus-Boelter	$Nu = 0.023 \cdot Re^{0.8} \cdot Pr^n$ $n = 0.4$ *for heating condition*	12.1 %	laminar
Gnielinski	$Nu = \dfrac{f/8 \cdot (Re - 1000) \cdot Pr}{1 + 12.7 \cdot \sqrt{(f/8)} \cdot (Pr^{0.66} - 1)}$ $f = 0.79 \cdot \ln(Re - 1.64)^{-2}$	4.11 %	turbulent

Fig. 8 – *Viscosity of CuO/water nano-fluid at different temperatures*

heat transfer coefficients. Accordingly, with increasing the heat and mass fluxes, the heat transfer coefficient dramatically increases, however, for regions with convective dominant mechanism the rate of increase is lower than that related to the region with dominant nucleate boiling heat transfer mecha-
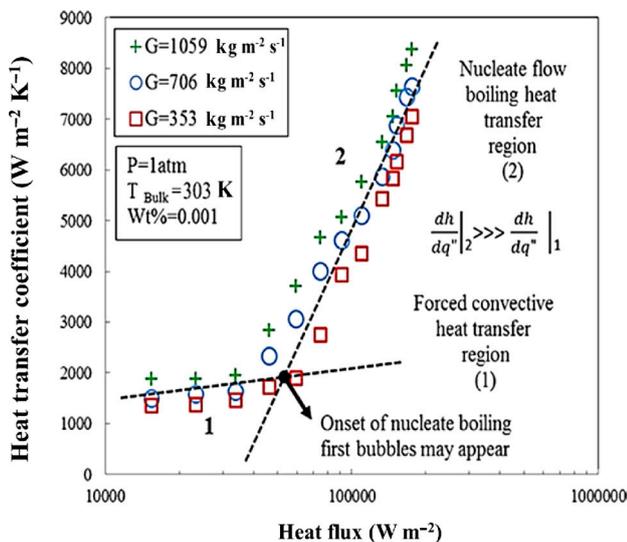

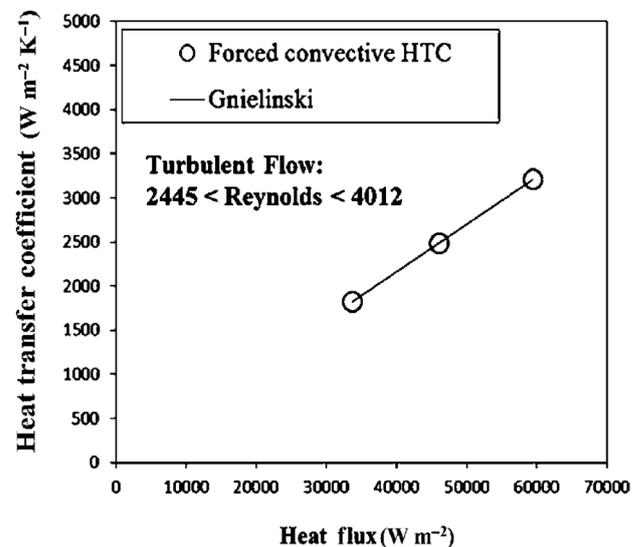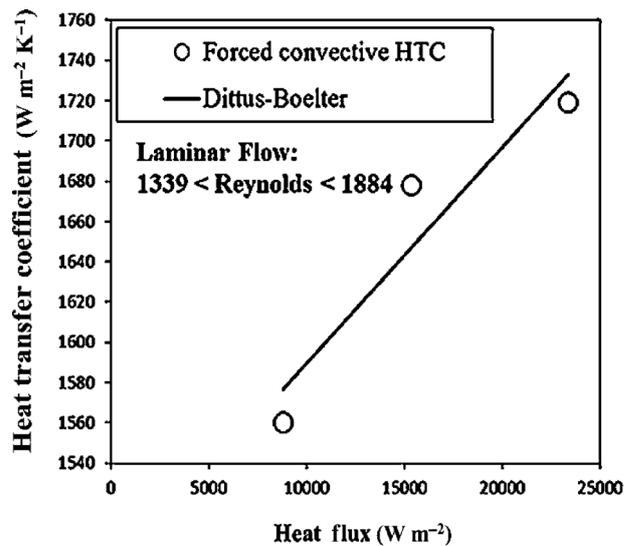Fig. 10 – *Influence of heat and mass flux on convective boiling heat transfer coefficients*

Fig. 9 – *Experimental results for deionized water in laminar and turbulent flow in comparison with well-known correlations*

nism. Fig. 10 presents the influence of heat and mass fluxes on flow boiling heat transfer. Note that, in nucleate boiling region, due to the bubble formation and bubble heat transport, the rate of heat transfer is intensified. In addition, bubble interaction can locally agitate the bulk of the nano-fluid around the heat-
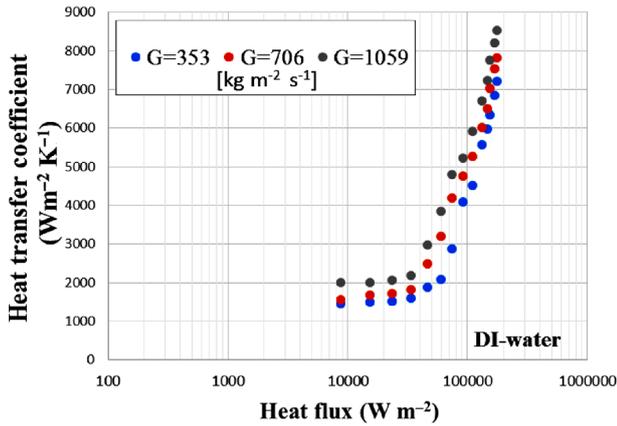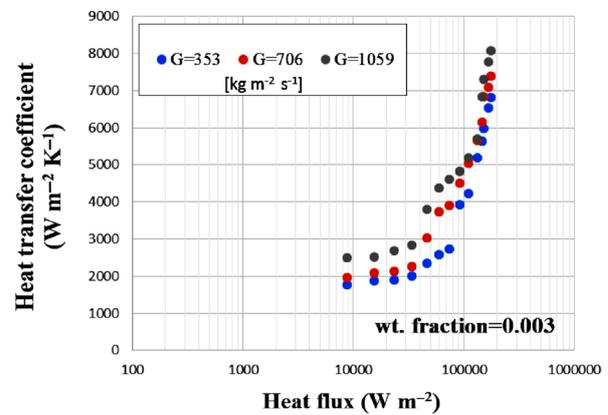
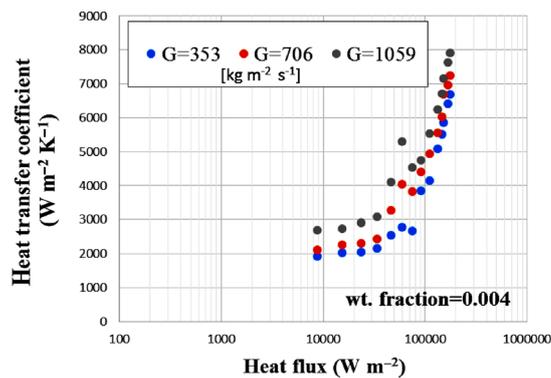(a) Flow boiling heat transfer coefficient of DI-water
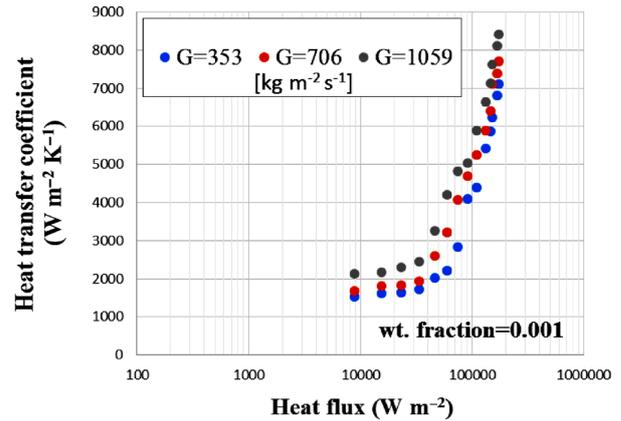
(b) Flow boiling heat transfer coefficient of CuO/water; wt. fraction: 0.001
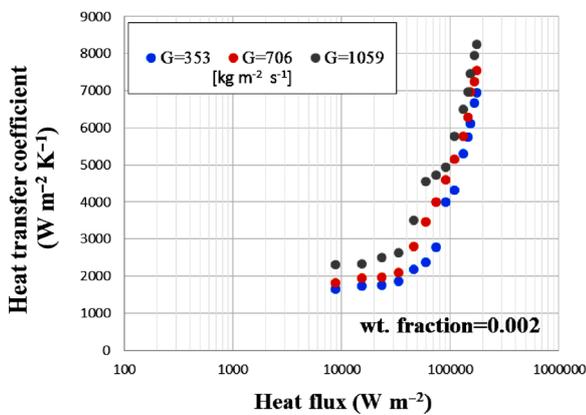
(c) Flow boiling heat transfer coefficient of CuO/water; wt. fraction: 0.002

(d) Flow boiling heat transfer coefficient of CuO/water; wt. fraction: 0.003

(e) Flow boiling heat transfer coefficient of CuO/water; wt. fraction: 0.004

Fig. 11 – *Influence of heat and mass flux on flow boiling heat transfer coefficient of CuO/water nano-fluid*

ing section which increases the heat transfer coefficient. For better understanding, the rest of the obtained results are also reported in Figs. 11(a-e).

Influence of concentration of nano-fluid

Experimental results demonstrate that concentration of nano-fluid has two significant roles in convective boiling heat transfer. For convection heat transfer region, a significant increase in heat transfer coefficient is reported, while for nucleate boiling heat transfer region, deterioration of heat transfer coefficient due to deposition and scale formation of nanoparticles on heating surface is registered. As can be seen in Fig. 12, when concentration of nanoparticles increases, force convective heat transfer coefficient dramatically increases, while for nucleate boiling heat transfer region

a deterioration of heat transfer coefficient is reported. This phenomenon is due to the scale formation and deposition of particles around the heating section and coating of these nanoparticles that change the surface properties and wettability of the heating surface. On the other hand, depositions will isolate the cavities and active nucleation sites, and reduce the number of nucleation sites, which subsequently causes the heat transfer to be reduced. Therefore, deterioration of heat transfer coefficient in nucleate boiling region can have a negative influence on heat transfer coefficient. The obtained results are in good agreement with those obtained experimentally in literature[25].
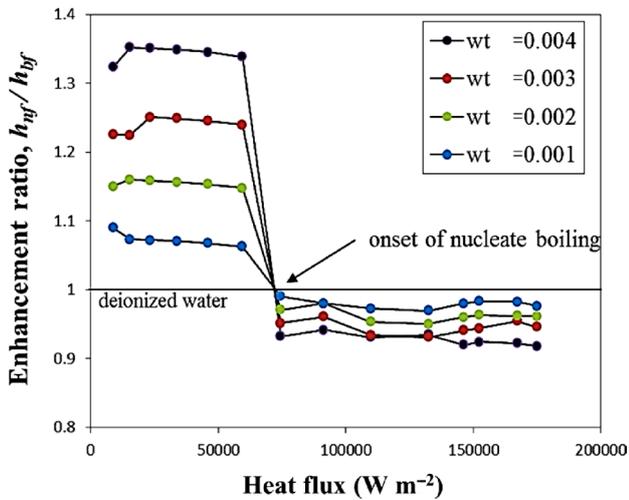

Fig. 12 – *Influence of concentration on convective boiling heat transfer coefficient of CuO/water nano-fluid (G=353 kg m⁻² s⁻¹ and sub-cooling level = 313 K)*

Influence of sub-coolingg level

In the present work, the most important influence of the inlet temperature, or sub-cooling level, can be seen on the inception heat flux. Inception heat flux is defined as the flux of heat in which the first observable bubble arises from the heated surface at sub-cooled boiling conditions. According to the experimental data, when sub-cooling level increases, the inception heat flux increases also. Briefly speaking, higher sub-cooling causes a significant time delay between end-point of force convective region and inception of nucleate boiling. In fact, at the higher sub-cooling temperature, higher inception heat flux is obtained.

Comparison with well-known correlations

Due to variation of mass flux (flow rate), Reynolds number varies in a wide range, and subsequently, laminar and turbulent flow can be observed during experiments. To validate the experimental data, the obtained results were compared to well-known correlations depending on the laminar or turbulent flow regimes or convective or nucleate boil-

ing heat transfer mechanisms. For laminar region in convective heat transfer area, Dittus-Boelter[26] correlation is employed, while for turbulent region, Gnielinski correlation[27] is used. For simplicity of representation of experimental data, no transient region is considered for flow regimes. For nucleate boiling zone, Rohsenow, Chen type model[28] and Gungor-Winterton well-known correlation[29] were used. Results of the comparison between these correlations and those obtained experimentally, indicate that good agreement is almost seen between experimental data and those obtained by correlations, except for Gungor-Winterton correlation in nucleate boiling zone, which shows a deviation of about 42.1 %. Figs. 13–15 show the results of comparisons between correlations and experimental
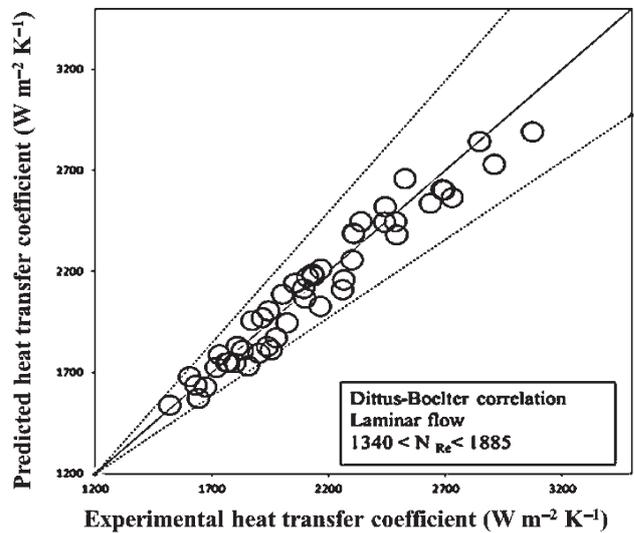

Fig. 13 – *Comparison between experimental data related to forced convection region and those obtained by Dittus-Boelter correlation in laminar flow*
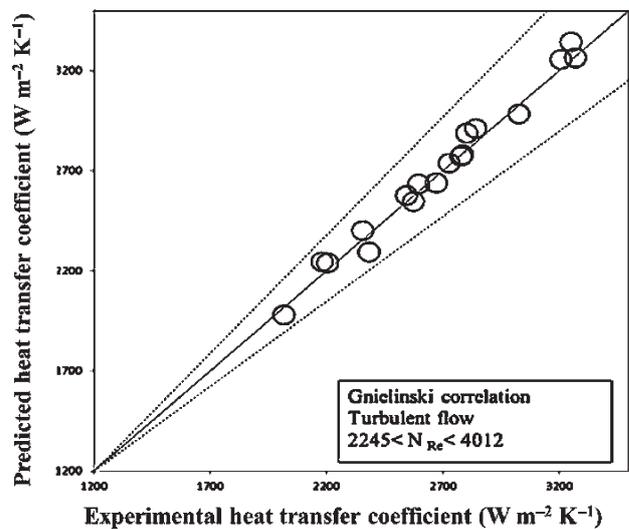

Fig. 14 – *Comparison between experimental data related to forced convection region and those obtained by Gnielinski correlation in turbulent flow*
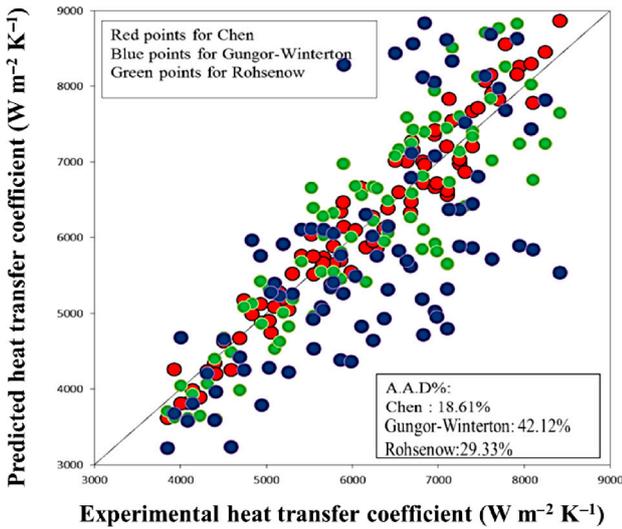
F i g . 1 5 – *Comparison between experimental data and well-known correlations (Chen model, Gungor-Winterton and Rohsenow) related to nucleate boiling region*

data, while Chen type model represents the reasonable values in comparison with other correlations with absolute average deviation of 18.6 % in comparison with 29.3 % and 42.1 % for Rohsenow and Gungor-Winterton correlations, respectively.

Conclusion

Studies on convective boiling heat transfer of dilute CuO water-based nano-fluids were experimentally conducted, and the following conclusions have been made:

i) For nano-fluid at wt. % = 0.004, and pH = 10.2, the longest stability was registered which is about 1080 h.

ii) During the experiments, two distinct heat transfer regions with different heat transfer mechanisms were observed, namely: force convective and nucleate boiling heat transfer regions.

iii) Heat and mass fluxes significantly increase the heat transfer coefficient in both regions of heat transfer. Influence of concentration of nano-fluid was interesting. In convective region, the heat transfer coefficient increased with the concentration of nano-fluids, while for nucleate boiling, due to deposition of particles around the heating surface, deterioration of heat transfer coefficient was observed.

iv) Comparisons between results and well-known correlations reveal that the Gungor-Winterton correlation was unable to predict the reasonable values for nucleate boiling heat transfer coefficient of nano-fluids. However, the Chen type model represents acceptable values with A.A.D % of about 18.61 % and is recommended for predicting the flow boiling heat transfer coefficient of nano-fluid.

N o m e n c l a t u r e s :

A – area, m^2
b – distance, m
C_p – heat capacity, J kg^{-1} ^{o}C^{-1}
G – mass flux, kg m^{-2} s^{-1}
h – heat transfer coefficient, W m^{-2} K^{-1}
k – thermal conductivity, W m^{-1} ^{o}C^{-1}
L – heater length, m
Pr   – Prandtl number
q – heat, W
q"   – heat flux, W m^{-2}
Re   – Reynolds number
s – distance between thermometer location and heat transfer surface, m
T – temperature, K
T_0 – Reference temperature = 298 K
V   – voltage, volt
x – liquid mass or mole fraction
$\dot{x}$ – vapour mass fraction
y – vapor mass or mole fraction

S u b s c r i p t s - S u p e r s c r i p t s

b   – bulk
bf   – base fluid
nf   – nano-fluid
fb   – flow boiling
in   – inlet
out   – outlet
l   – liquid
nb   – nucleate boiling
sat   – saturated
th   – thermometers
v   – vapor
w   – wall
wt.   – weight fraction

G r e e k   s y m b o l s

α – heat transfer coefficient, W m^{-2} K^{-1}
ρ – density, kg m^{-3}
μ – viscosity, kg m^{-1} s^{-1}
κ – Boltzmann constant = 1.381 $\cdot$10^{-23}, J K^{-1}
ϕ – sphericity, see Table 2
φ – volume fraction of particles

References

1. *Barber, J., Brutin, D., Tadrist, L.*, A review on boiling heat transfer enhancement with nano-fluids, Nanoscale Res. Lett. **6** (2011) 280.
   doi: http://dx.doi.org/10.1186/1556-276X-6-280

2. *Choi, S.*, Enhancing thermal conductivity of fluids with nanoparticles, Proceedings of the ASME International Mechanical Engineering Congress and Exposition, San Francisco, (1995), pp 99–105.

3. *Yu, W., France, D., Routbort, J., Choi, S.*, Review and comparison of nano-fluid thermal conductivity and heat transfer enhancements, Heat Trans. Eng. **29** (2008) 432.
   doi: http://dx.doi.org/10.1080/01457630701850851

4. *Lee, J. K., Hwang, Y. J., Ahn, Y. C., Shin, H. S., Lee, C. G., Kim, G. T., Park, H. S.*, Investigation on characteristics of thermal conductivity enhancement of nano-fluids, Curr. Appl. Phys. **6** (2006) 1068.
   doi: http://dx.doi.org/10.1016/j.cap.2005.07.021

5. *Faulkner, D., Khotan, M., Shekarriz, R.* Practical design of a 1000 W/cm² cooling system (high power electronics). Semiconductor Thermal Measurement and Management Symposium (Nineteenth Annual IEEE), USA, (2003), 223.

6. *Lee, J., Mudawar, I.*, Assessment of the effectiveness of nano-fluids for single-phase and two-phase heat transfer in micro-channels, Int. J. Heat Mass Trans. **50** (2007) 452.
   doi: http://dx.doi.org/10.1016/j.ijheatmasstransfer.2006.08.001

7. *Peng, H., Ding, G., Jiang, W., Hu, H., Gao, Y.*, Heat transfer characteristics of refrigerant-based nano-fluid flow boiling inside a horizontal smooth tube, Int. J. Refrigeration **32** (2009) 1259.
   doi: http://dx.doi.org/10.1016/j.ijrefrig.2009.01.025

8. *Peng, H., Ding, G., Jiang, W., Hu, H., Gao, Y.*, Measurement and correlation of frictional pressure drop of refrigerant-based nano-fluid flow boiling inside a horizontal smooth tube, Int. J. Refrigeration **32** (2009) 1756.
   doi: http://dx.doi.org/10.1016/j.ijrefrig.2009.06.005

9. *Boudouh, M., Gualous, H., Labachelerie, M.*, Local convective boiling heat transfer and pressure drop of nano-fluid in narrow rectangular channels, App. Therm. Eng. **30** (2010) 2619.
   doi: http://dx.doi.org/10.1016/j.applthermaleng.2010.06.027

10. *Kim, S. J., McKrell, T., Buongiorno J., Hu, L.*, Subcooled flow boiling heat transfer of dilute alumina, zinc oxide, and diamond nano-fluids at atmospheric pressure, Nuclear Eng. Des. **240** (2010) 1186.
    doi: http://dx.doi.org/10.1016/j.nucengdes.2010.01.020

11. *Kim, T., Jeong, T., Chang, S.*, An experimental study on CHF enhancement in flow boiling using Al2O3 nano-fluid, Int. J. Heat Mass Trans. **53** (2010) 1015.
    doi: http://dx.doi.org/10.1016/j.ijheatmasstransfer.2009.11.011

12. *Henderson, K., Park, Y., Liu, L., Jacobi, A.*, Flow-boiling heat transfer of R-134a-based nano-fluids in a horizontal tube, Int. J. Heat Mass Trans. **53** (2010) 944.
    doi: http://dx.doi.org/10.1016/j.ijheatmasstransfer.2009.11.026

13. *Das, S. K., Putra, N., Roetzel, W.*, Pool boiling characteristics of nano-fluids, Int. J. Heat Mass Transfer **46** (2003) 851.
    doi: http://dx.doi.org/10.1016/S0017-9310(02)00348-4

14. *Ahn, H. S., Kim, H., Jo, H., Kang, S., Chang, W., Kim, M. H.*, Experimental study of critical heat flux enhancement during forced convection flow boiling of nano-fluid on a short heated surface, Int. J. Multiphase Flow **36** (2010) 375.
    doi: http://dx.doi.org/10.1016/j.ijmultiphaseflow.2010.01.004

15. *Sarafraz, M. M., Peyghambarzadeh, S. M., Alavi Fazel, S. A., Vaeli, N.*, Nucleate pool boiling heat transfer of binary nano mixtures under atmospheric pressure around a smooth horizontal cylinder, Periodica Polytechnic, Chemical Engineering **56** (2012) 1.

16. *Sarafraz, M. M., Pyghambarzadeh, S. M.*, Nucleate Pool Boiling Heat Transfer to Al₂O₃-Water and TiO₂-Water Nano-fluids on Horizontal Smooth Tubes with Dissimilar Homogeneous Materials, Chem. Biochem. Eng. Q. **26** (2012) 199.

17. *Sarafraz, M. M., Hormozi, F.*, Application of thermodynamic models to estimating the convective flow boiling heat transfer coefficient of mixtures, Exp. Thermal Fluid Sci. **53** (2014) 70.
    doi: http://dx.doi.org/10.1016/j.expthermflusci.2013.11.004

18. *Sarafraz, M. M., Hormozi, F.*, Convective boiling and particulate fouling of stabilized CuO-ethylene glycol nano-fluids inside the annular heat exchanger, Int. Commun. Heat Mass Trans. **53** (2014) 116.
    doi: http://dx.doi.org/10.1016/j.icheatmasstransfer.2014.02.019

19. *Sarafraz, M. M., Hormozi, F.*, Scale formation and subcooled flow boiling heat transfer of –water nano-fluid inside the vertical annulus, Exp. Thermal Fluid Sci. **52** (2014) 205.
    doi: http://dx.doi.org/10.1016/j.expthermflusci.2013.09.012

20. *Seara, J. F., Uhia, F. J., Sieres, J.*, Laboratory practices with the Wilson plot method, Exp. Heat Trans. **20** (2007) 123.
    doi: http://dx.doi.org/10.1080/08916150601091415

21. *Kline, S. J., McClintock, F. A.*, Describing uncertainties in single-sample experiments, Mech. Eng. **75** (1953) 3.

22. *Sarafraz, M. M., Peyghambarzadeh, S. M.*, Experimental study on subcooled flow boiling heat transfer to water–diethylene glycol mixtures as a coolant inside a vertical annulus, Exp. Therm. Fluid Sci. **53** (2013) 154.
    doi: http://dx.doi.org/10.1016/j.expthermflusci.2013.06.003

23. *Peyghambarzadeh, S. M., Sarafraz, M. M., Vaeli, N., Ameri, E., Vatani, A., Jamialahmadi, M.*, Forced convection and sub-cooled flow boiling heat transfer to pure water and n-heptane in an annular heat exchanger, Annal Nuc. En. **53** (2013) 401.
    doi: http://dx.doi.org/10.1016/j.anucene.2012.07.037

24. *Sarafraz, M. M., Peyghambarzadeh, S. M., Vaeli, N.*, Subcooled flow boiling heat transfer of ethanol aqueous solutions in vertical annulus space, Chem. Ind. Chem. Eng. Q. **18** (2012) 315.
    doi: http://dx.doi.org/10.2298/CICEQ111020008S

25. *Sarafraz, M. M., Hormozi, F., Kamalgharibi, M.*, Sedimentation and convective boiling heat transfer of CuO-water/ethylene glycol nano-fluids, Heat Mass Trans. **50** (2014) 1237.
    doi: http://dx.doi.org/10.1007/s00231-014-1336-y

26. *Dittus, F. W., Boelter, L. M. K.*, Heat transfer in automobile radiators of the tubular type, University of California Publications in Engineering **2** (1930) 443.

27. *Gnielinski, V.*, Wärmeübertragung in Rohren, VDI Wärmeatlas, (fifth ed.), VDI-Verlag, Düsseldorf, 1986, pp 345–410.

28. *Chen, J. C.*, A correlation for boiling heat transfer to saturated fluids in convective flow, Ind. Eng. Chem. Process Design Dev. **5** (1966) 322.
    doi: http://dx.doi.org/10.1021/i260019a023

29. *Gungor, K. E., Winterton, H. S.*, A general correlation for flow boiling in tubes and annuli, Int. J. Heat Mass Trans. **29** (1986) 351.
    doi: http://dx.doi.org/10.1016/0017-9310(86)90205-X

30. *Fedele, L., Colla, L., Bobbo, S., Barison, S., Agresti, F.*, Experimental stability analysis of different water-based nano-fluids, Nanoscale Res. Letter **6** (2011) 300.
    doi: http://dx.doi.org/10.1186/1556-276X-6-300